

## THE STRUCTURE OF TURBULENT JETS

**Emil Sekula, José M. Redondo**

**Departament de Física Aplicada, Universitat Politècnica de Catalunya, Barcelona, Spain**

### **Abstract**

Present work shows some results of research on turbulent jets and plumes, their structures and effects occurred in different configurations (free jet, wall jet, 'bubbly' jet). The proposed work is based principally on experiments but there are also made some comparisons between experimental and environmental observations. We discuss here in summary the series of detailed experiments that have been performed in laboratory utilizing visualizations methods (Particle Image Velocimetry) and Acoustic Doppler Velocimeter (ADV) measurements of turbulence parameters in order to obtain a basic understanding of the turbulence phenomenon. We aim to understand the behaviour of turbulent jets incorporating the recent advances in non-homogeneous turbulence, structure function analysis, multifractal techniques and extended self-similarity.

One of the used configurations is the turbulent wall jet that occurs often in several environmental and industrial processes such as aeronautics design, heating, cooling, ventilation and environmental fluid dynamics. Other one is a 'bubbly' jet, a kind of jet 'filled' with bubbles. We used also two kinds of jet's sources: two pumps with smaller and bigger flow rate and different Reynolds numbers.

Results contain both measured (mean and fluctuation velocities, amplitudes, signal-noise-ratio, etc.) and statistical values obtained with provided and also personally created programs (correlations, covariance, kurtosis, standard deviation, skewness) and other such Reynolds number or turbulence intensity. We focus special attention on correlations and structure function which are useful for energy spectra analysis. It is interesting to investigate the convergence of performed experiments with Kolmogorov theory taking into account non-homogeneity, non isotropy, etc. and to use Extended Self Similarity (ESS) and the third order structure functions to investigate the scale to scale transfer of energy.

With deep analysis of the performed results we can judge the adaptation of measurement methods and acquire more experience with its application.

An additional part of the work includes multi-fractal analysis of Synthetic Aperture Radar (SAR) images of the sea surface. The multi-fractal method allows investigating the turbulent and fractal structure of non homogeneous jets affected by different levels of turbulence. Other aims of the investigation under way are to determine the structure of ocean surface detected jets and compare coastal and boundary effects on the structure of river jets. A useful outcome is to develop further multi-fractal techniques useful for environmental monitoring in space.

We perform the box counting algorithm for the different intensities of vortices detected by SAR using special program Ima\_Calc. SAR images allow us to observe convective cells and vortices formed in the sea surface.

## **Introduction**

Most practical flows occurring in nature and in engineering applications involve non-homogeneous turbulent flows. Great progress has been made in the last century (since Kolmogorov's work K41 and K62 theories <sup>(6), (7)</sup>) on the structure and theory of homogeneous and isotropic turbulence, but non-homogeneous or boundary affected flows still lack a comprehensive theory, Mahjoub (2000) <sup>(11)</sup>.

The mechanics of the turbulent jets, although studied during the last decades, still is a paradigm of flow behaviour, together with wakes and boundary layers, and all these flows are of great interest to researchers. In recent years, thanks to improved remote sensing and non intrusive Doppler velocimeters we can observe concentration on the environment and laboratory flows, for example dilution and mixing of pollutants in water bodies at many scales. Studies of the behaviour of relatively basic kind of jets (the free turbulent jet, wall jet, buoyant jets and plumes) are very important for the understanding of more complex configurations. The investigation of the above mentioned kinds of flow have been performed during many years aiming mostly at the mean flow predictions but there are still some important unsolved questions in the behaviour of the turbulent cascades and their structure because of the past limits of measurements methods <sup>(8), (9)</sup>.

We aim to understand the behaviour of turbulent jets incorporating the recent advances in non-homogeneous turbulence, structure function analysis, multifractal techniques and extended self-similarity.

Using on the same experiments more than one method of diagnostic allows us to compare results and improve the understanding of the flows and of the laboratory techniques, this is also an important argument for network based research because the new experimental techniques implemented (e.g. LIF, PIV, Particle Tracking, Fractal analysis, intermittency, structure function analysis, etc) may be useful to other researchers in experimental fluid dynamics or in related fields.

Different experiments have been previously done with turbulent jets. We present here measurements on the turbulent structure of wall-jet flows including spectral measurements of the non-homogeneous turbulent cascade processes and thus complement previous experiments, which were mostly concerned with mean structure. Hinze (1975) <sup>(3)</sup> described transport processes in turbulent flows, free turbulent shear flows and "wall" turbulent shear flows. A basic description of turbulent jets cited in Rajaratnam (1976) <sup>(13)</sup> or the scaling differences between plane jets and measurements in radial wall jets are discussed by Knowles, et al. (1998) <sup>(5)</sup> confirming axisymmetry in round, turbulent jets impinging normally on a flat plate and self-similarity in the velocity profiles. Similar research works cited in the Annual Review of Fluid Mechanics <sup>(8), (9)</sup> discuss engineering details and particular cases. The important role of body forces involving plumes/buoyant jets is described in Jirka (2004) <sup>(4)</sup>, especially information about integral models for the analysis and prediction of turbulent buoyant jets.

There are many other research works and results describing different aspects of wall-jet flows, but they in majority use as a fundamental Kolmogorov's theory <sup>(6), (7)</sup>. Considering the new advances in non-homogeneous turbulent structure (Castilla, 2001 <sup>(1)</sup>, Mahjoub (2000) <sup>(11)</sup>) we show new measurements that will help to understand the role of turbulent cascades when affected by coherent structures.

### Experimental setup

We have used 3 kinds of jets using different configuration and sources (pumps with different flow rates) and changing also Reynolds numbers (velocities of the jets and diameters of nozzles). The jets were generated in about 4 m long Perspex tank with a recirculating pump system. The co-ordinate system and the measuring stations are shown on Figure 1. There is pure water with some particles in the tank. The jets are water jets so we do not have density difference. One of the set up includes also buoyancy induced by air bubbles dissolved in the flow, we call it here 'bubbly' jet. Temperature of the water is about 20-25 Celsius degrees so we can assume it as room temperature. The ADV measuring probe was placed 5 cm over axis of the jet so measurements could be made along the jet centreline as well as at different distances from the wall without jet disturbance.

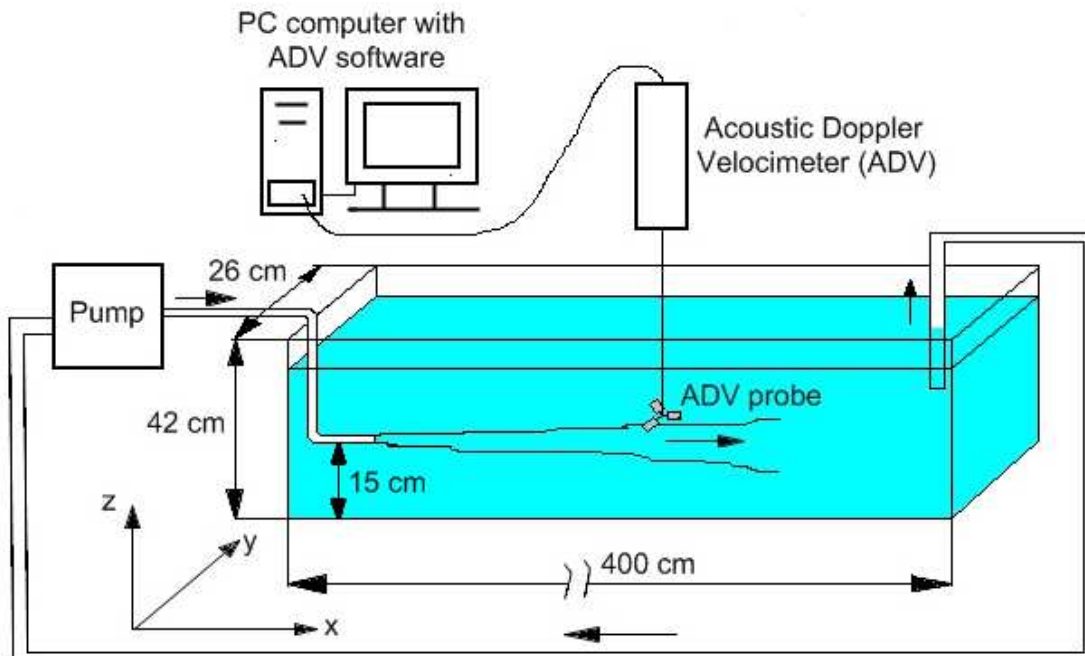


Figure 1. Experimental configuration.

Measurements were made for different distances between the jet and the wall (coordinate  $y$ ).

The flow parameters for both experiments were:

- a) Small pump: mass flow:  $Q = 64 \text{ cm}^3/\text{s}$ , stream's velocity:  $V = 32 \text{ cm/s}$ , diameter of the nozzle:  $d = 1,6 \text{ cm}$ ;
- b) Big pump:
  - b1) water jet, mass flow:  $Q = 524,6 \text{ cm}^3/\text{s}$ , stream's velocity:  $V = 552,3 \text{ cm/s}$ , diameter of the nozzle:  $1,1 \text{ cm}$ ;
  - b2) "buoyant bubbly jet", mass flow:  $Q = 645 \text{ cm}^3/\text{s}$ , stream's velocity:  $V = 205 \text{ cm/s}$ , diameter of the nozzle:  $2 \text{ cm}$ .

The SonTek ADV shown in Figure 2, was used for the detailed turbulence measurements, is a versatile, high-precision instrument used to measure 3D water

velocities. The ADV uses acoustic Doppler technology to measure 3D flow in a small sampling volume located a fixed distance (in our case 5 cm) from the probe. Voulgaris et al. <sup>(16)</sup> described the evaluation of ADV for turbulence measurements assuring a good resolution at the used Re.



Figure 2. Acoustic Doppler Velocimeter (ADV) and 3D probes.

We measured turbulence parameters in different points of the jet zone and outside. The measurements were done during periods of 15 minutes (900 s) at each point, the long measuring periods, longer than in previous experiments, were specially designed for the structure function and higher order momentum and probability distribution function analysis. Sampling rate is 25 Hz so we have for each point of measurements 22500 data samples.

### **Results of experiments**

The basic direct measured parameters have been: the three velocity components, standard deviation, kurtosis, skewness and covariance (measure of the correlation between two velocity components). Majority of them are statistical terms and there are useful to analyse results of our investigation. Here we will discuss just some of them.

#### Standard deviation

Standard deviation of the samples is equal to the RMS turbulence (the root-mean-square of the turbulent velocity fluctuations or the square root of the mean of the deviations from the mean velocity). ADV software computes the sample standard deviation. For example, the RMS turbulence for the x velocity component is:

$$RMS[V_x'] = \sqrt{(V_x')^2} = \sqrt{\frac{\sum V_x^2 - (\sum V_x)^2 / n}{n-1}}$$

We can observe in Figure 3 the decrease of R.M.S. velocity for three components (x, y and z) with distance from the nozzle (source of the jet). Highest values correspond to the x and y direction both because of the higher vertical vorticity induced by the side

wall and because of the lower spatial resolution of the z component. We can note the peaks of R.M.S. velocity for the x and y directions between 10 and 20 x/D caused by the wall effect that produces higher vorticity and also higher shear in the turbulent velocities

(related to the dissipation as  $\varepsilon = \nu \overline{\left(\frac{du'}{dx}\right)^2}$  of the turbulent velocity fluctuations) and we

can observe where boundary layer interaction with the jet appears. Comparing the two figures (y = 4 cm and y = 13 cm) we can observe that in y = 4 cm (wall jet) case the effect of the wall interaction is much larger.

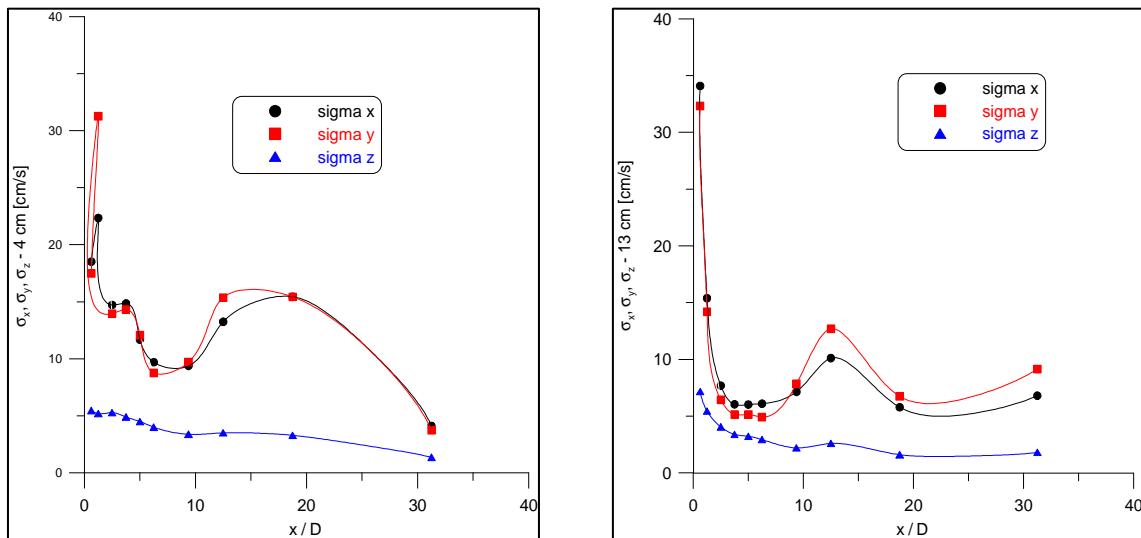


Figure 3. Standard deviation versus non dimensional distance function (x/D) for two cases of the jet: y = 4 cm and y = 13 cm (small Reynolds number).

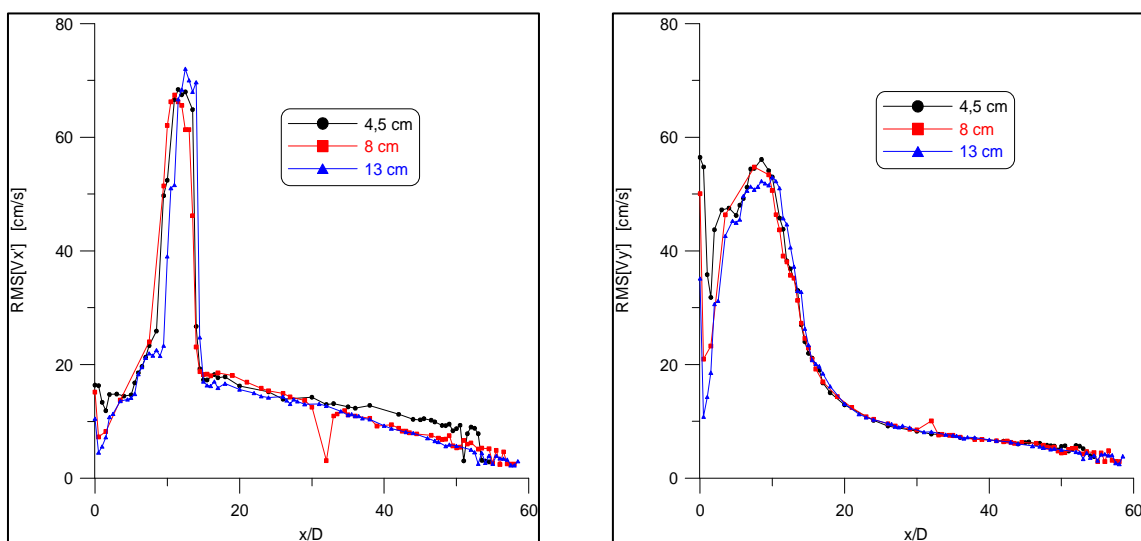


Figure 4. Standard deviation x and y for three distances from the wall versus non-dimensional distance x/D (“bubbly” jet case).

Comparing results of R.M.S velocity of “bubbly” jet case (Figure 4) we can notice that effect of the wall is noticeable (large peak of the curve near the value  $x/D = 12$ ) but we can not notice the difference between three distances from the wall, it is not so well apparent like in low Reynolds number normal jet case. Probable causes of this are higher outlet velocity in “bubbly” jet case (about 6 times) and effect of the bubbles. The same observations are visible in  $y$  – component or R.M.S. turbulence but values are smaller. In normal jet case (Figure 5) the difference in R.M.S. between the three distances from the wall are more evident.

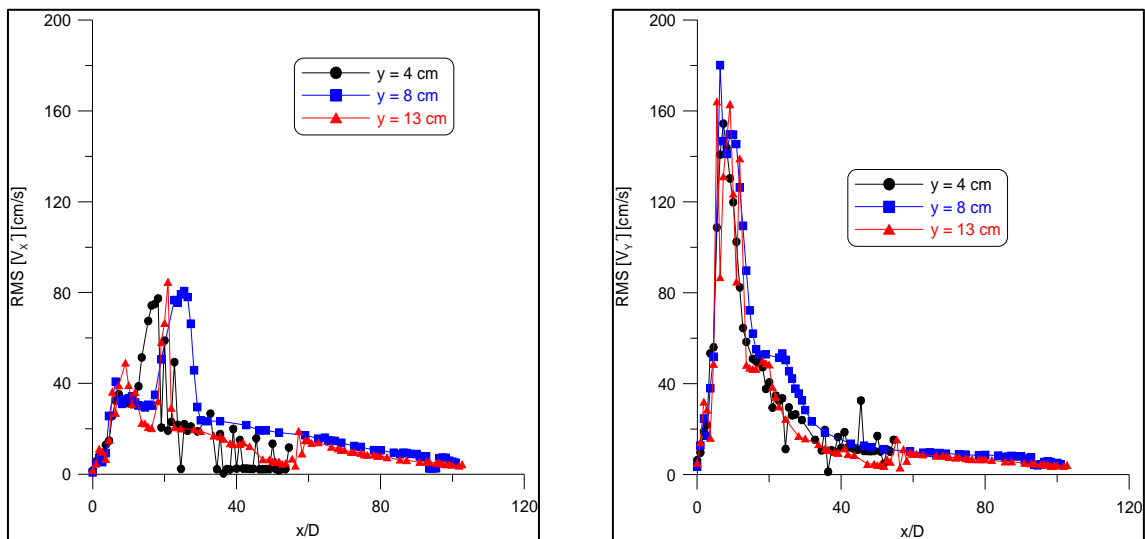


Figure 5. Standard deviation  $x$  and  $y$  for three distances from the wall versus non dimensional distance  $x/D$  (normal jet case).

#### Power spectrum and Probability Distribution Function (PDF)

In Figure 6 we show the amplitude of the Fast Fourier Transforms (using the logarithm described in Press, Flannery, Teukolsky, Vetterling (1989)) of the velocity data for three distances from the nozzle ( $x = 1$  cm,  $x = 38$  cm and  $x = 62$  cm) for normal jet case together with the PDF functions for the  $x$  and  $y$  turbulent velocity components. They are two statistical description of the turbulence.

The much wider pdf distribution at 38 cm proves that the wall jet interaction is a mayor source of turbulence; at this particular location it seems that a vortex roll up produces a recirculating flow. At a further downstream location the mean velocities tend to zero and the PDF's narrows.

The slope of the energy spectra is seen to decrease at the intermediate measuring station ( $x = 38$  cm), this reflects the increase in intermittency produced by the strong interaction between the jet and the wall. At the first station ( $x = 1$  cm) a more no homogeneous turbulent flow, but at very different Reynolds numbers, produces a more local cascade with less intermittency. Note that the turbulent cascade only takes place between 0.2 Hz and 8 Hz as higher frequencies show signs of aliasing.

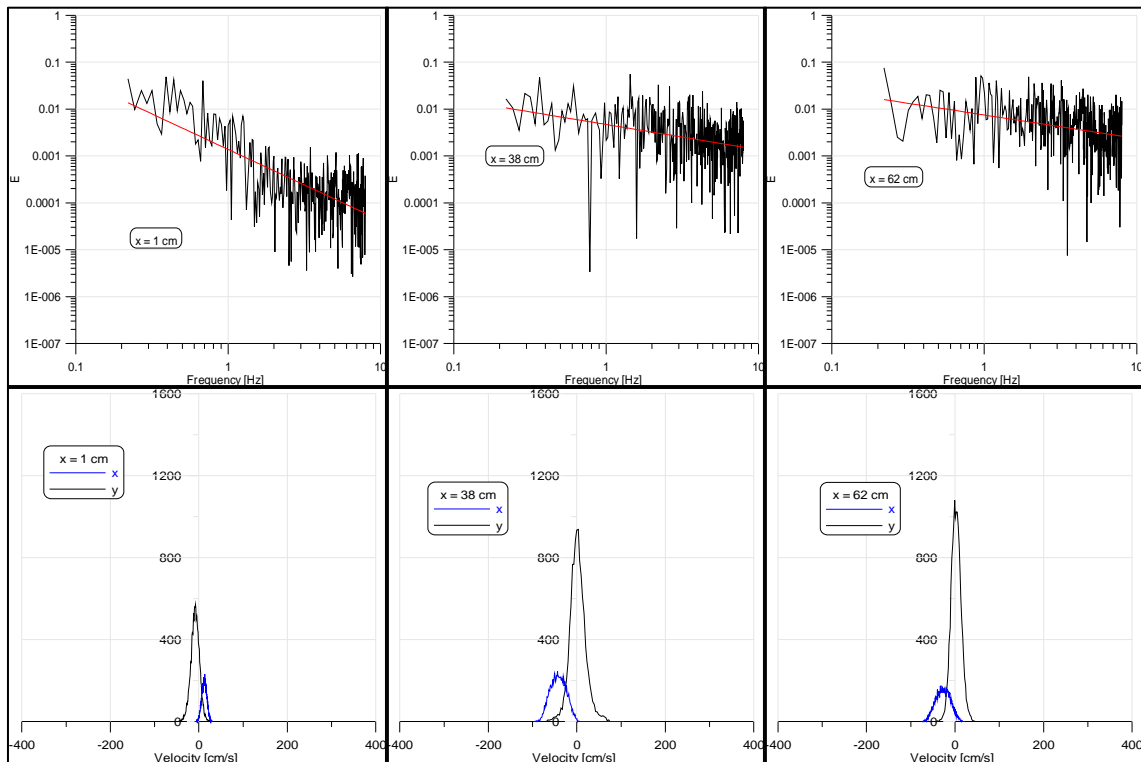


Figure 6. Power spectrum of signal amplitude and Probability Distribution Function (PDF) of velocity for three distances from the nozzle  $x = 1, 38$  and  $62$  cm (normal jet case,  $y = 4$  cm).

### Correlations

A correlation score is calculated for each sample stored in the ADV file, for each of the three signal beams; values are expressed in percent, with 100 being a perfect correlation. Correlations of 70 to 100 percent are typically considered good. Low correlation values may indicate problems related to turbulence, signal strength, scattered density, excessive air bubbles, or problems with the probe itself.

Results of correlations are presented on Figure 7.

We can observe that in both cases the correlation score is less than recommended 70 % in first zone of the jet (in normal jet it is about  $x/D = 50$  and in ‘bubbly’ jet about  $x/D = 22$ ). It can indicate problems related to turbulence and air bubbles in both cases. However it is proven that in some situations in which COR values much less than 70 % results were the best we could get, and yet the velocity data seemed to be accurate, judging from their correlation with other independent measurements and their consistency with ADV data from adjacent areas of the flow in which we could get  $COR > 70$  %. It can be difficult to obtain  $COR > 70$  % in highly turbulent flows that are near the upper limit of the velocity range setting for the ADV. This indicates that good velocity measurements can be obtained even when the correlation is low. We can verify our results using other parameter: Signal-To-Noise Ratio (SNR) is the ratio of signal strength to the background acoustic noise level inherent in the ADV instrument. We could try also to filter our data series using adequate filtering method. The correlation score is a useful parameter to prove correctness of ADV results.

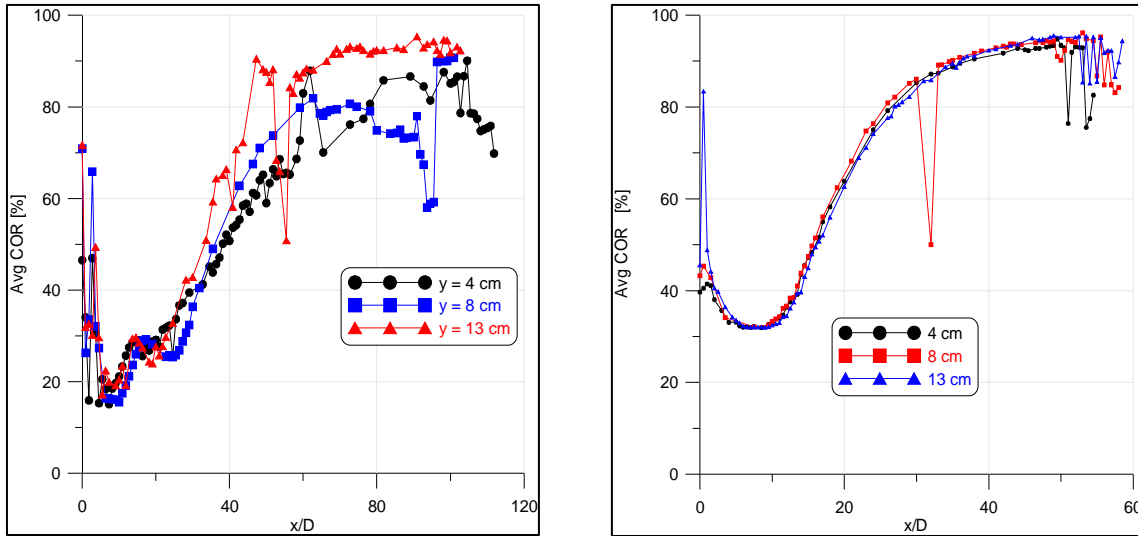


Figure 7. Correlations for normal (left) and ‘bubbly’ (right) jets for different distances from the wall.

#### Autocorrelation

In a time series, the relationship between values of a variable taken at certain times in the series and values of a variable taken at other, usually earlier times.

We calculate autocorrelation for x and y velocity component.

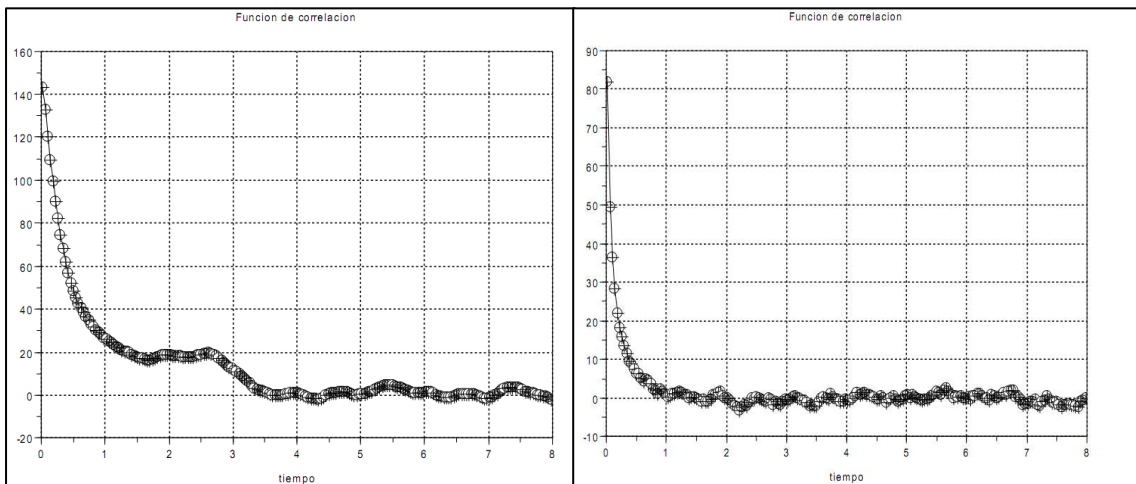


Figure 8. Autocorrelation for x (left) and y (right) velocity component for normal jet case,  $x = 84$  cm,  $y = 4$  cm.

Analysing Figure 8 we can observe in x component case that from 2 s appears an increment of the correlation but if we interpolate the initial curve to find the point where the correlation is 0 we have 3,5 s (without interpolating we have also 3,5 s). In y velocity component case we have 1 s so we have good resolution of data capture (in 1 s – 25 data). X – component shows that the majority of turbulence is in x – direction and its dissipation is slower.

**Structure functions**

The velocity structure functions of order p are defined in terms of the moments of velocity differences as:

$$S_p(l) = \left\langle \left( u(\vec{x} + \vec{l}) - u(\vec{x}) \right)^p \right\rangle = \left\langle (\delta u_l)^p \right\rangle$$

Where  $\langle \dots \rangle$  signify ensemble average and u is the velocity component parallel to  $\vec{l}$ .

Especially the third-order structure function of the velocity (Figure 9) is important for our contemplation. It is proportional to the separation distance l in the inertial range of Energy spectra and it is standard procedure in the analysis to define an inertial range. But this is predicted by Kolmogorov theory (1941) and in non-homogenous and non-isotropic turbulence this proportionality is not warrantable. That is why is so interesting compare third-order structure function but also absolute scaling exponent, relative scaling exponent and intermittency parameter. Detailed information about this problem contains work of Mahjoub (2000) <sup>(11)</sup>.

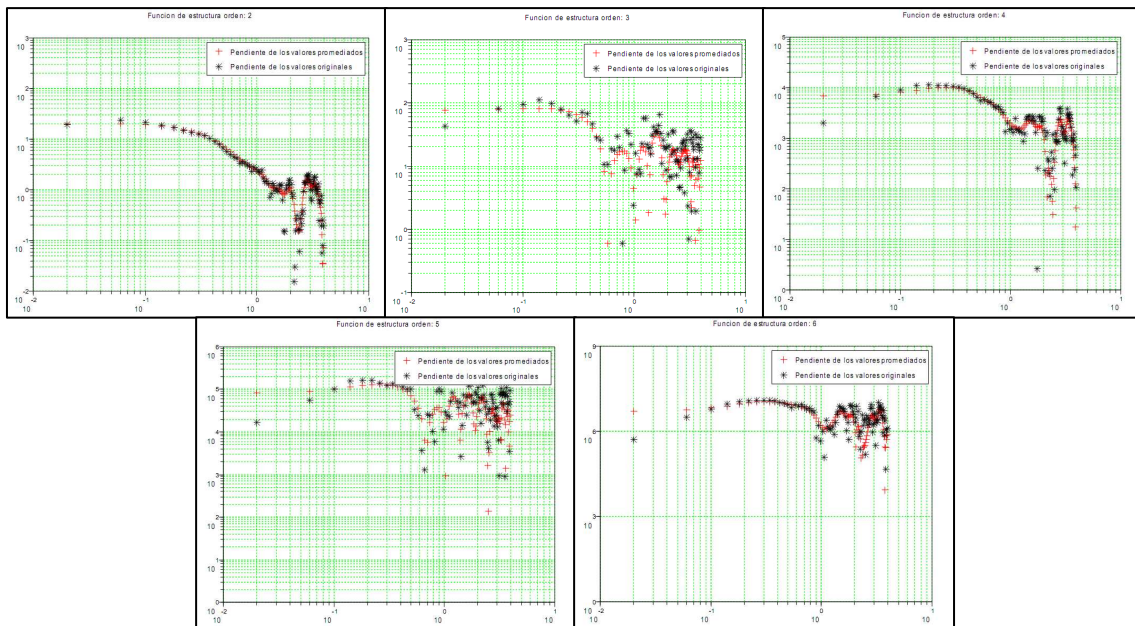


Figure 9. Structure functions of p = 2, 3, 4, 5 and 6 order respectively for normal jet case, x = 84 cm, y = 4 cm.

**Multifractal analysis of the vortical structures using Synthetic Aperture Radar (SAR) images.**

Most of the SAR images analyzed were obtained during 1996-1998. North-East part of Mediterranean Sea (Balearic Sea, Catalan Cost) were taken into consideration. Resolution of the one image is 2361 x 2419 pixels (about 100 km x 100 km). We selected parts of these images in order to analyse vertical structures of the sea surface. On the Figure 10 it is shown part of the one of SAR image with marked zones of interest.

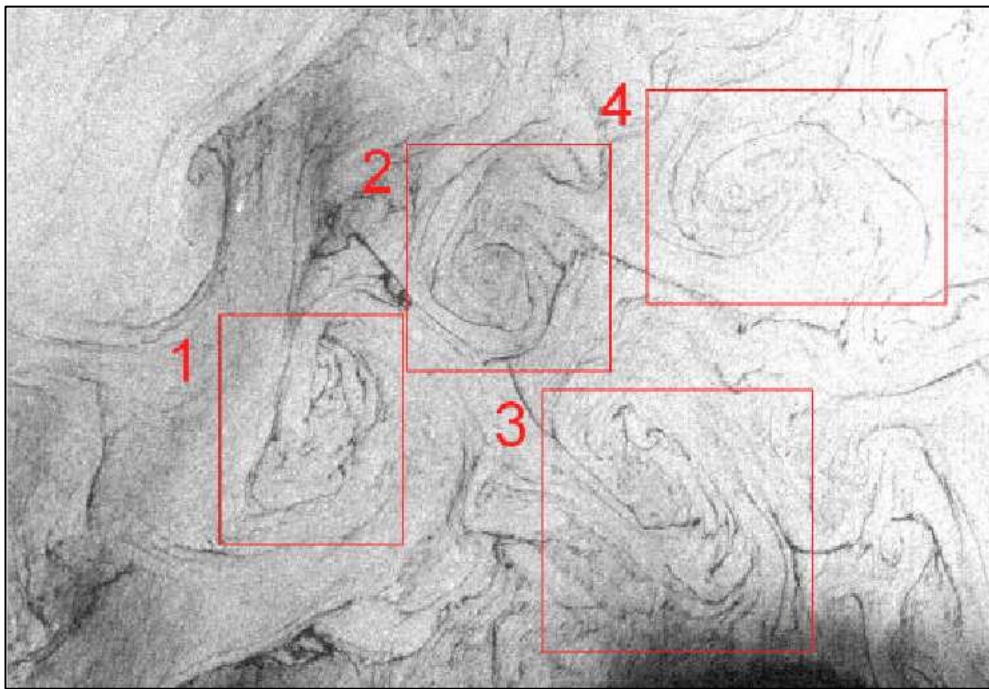


Figure 10. Part of SAR image with marked sea vortices.

In order to distinguish the different types of features in the ocean surface, it is possible to apply fractal and multi - fractal analysis. This method is described more detailed in Platonov et al. (2007) <sup>(12)</sup>. Simply generalising we perform the box counting algorithm for the different intensities of vortices detected by these images. In the sea surface we can observe sea vortices (Figure 11, top – left) but also typical regions for SAR signatures where convective cells are formed (bottom – left). It is interesting to compare the multifractal appearance of the different signatures and this is shown for these two examples in Figure 11.

The quite different fractal structure of the convective cells has a clear plateau of a constant value of the maximum fractal dimension indicates that this measure is the same for the different intensity values of the SAR images. On the other hand, the vertical structures exhibit a slightly higher fractal value (1.7) for the higher SAR reflectivity (white) and a linear increase from the darker features. It is obvious that the dark features, being elongated and smoother have a smaller fractal dimension than the background area between the spiral structures. But the appearance of a linear increase is not clear. The fact that convective structures take place in all the images and the structures are marked both by darker (meaning a smooth surface) and white (rougher sea surface areas) as shown by the histogram sequence in Figure 12, explains that at a wider range the maximum fractal dimension  $D$  is about the same (1,55) for convective cells.

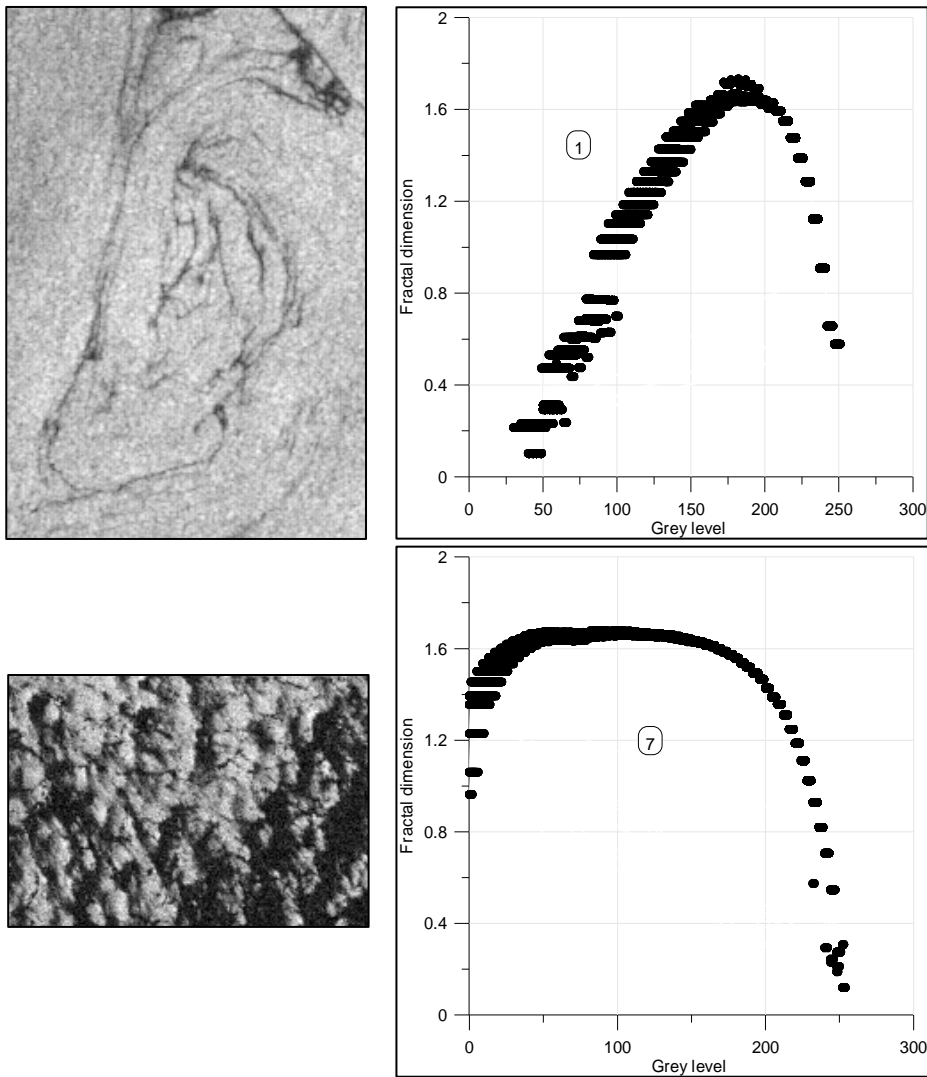


Figure 11. Multifractal structure of vortex 1 of Figure 10 (top right) and a convective region (bottom right).

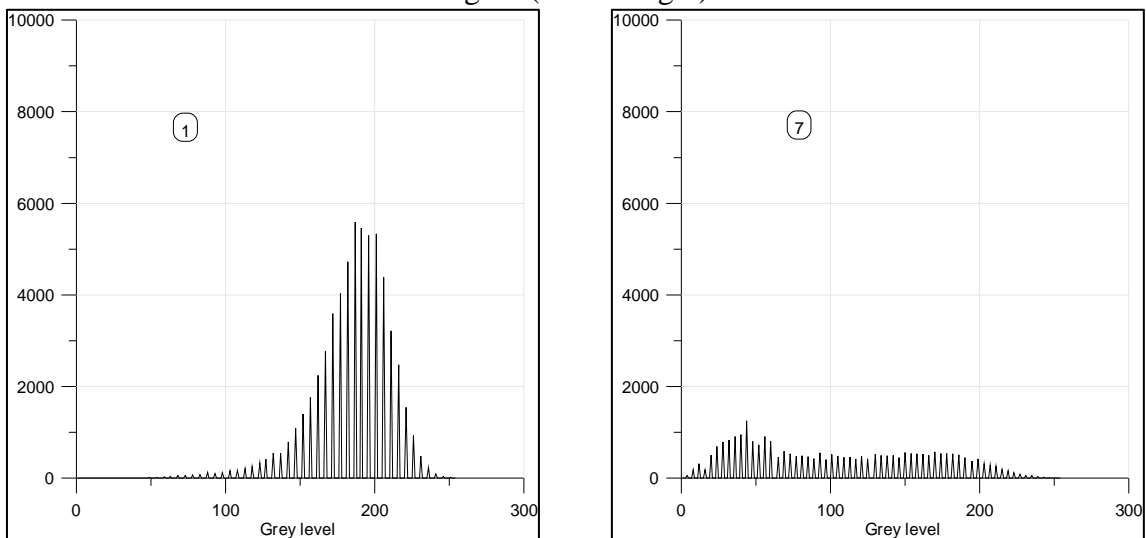


Figure 12. Histogram distributions of vortex 1 of Figure 10 (left) and a convective (right).

## **Conclusions**

The main objective of this paper is to show the investigation phase of our work on the structure of turbulent jets (especially wall jets) and interactions with boundary non-homogeneities together with mixing effects in experimental flow fields. Work is based on detailed experiments using ADV measurements. The initial experimental configurations have provided information about the characteristics of the turbulent free jet, the circular jet and the turbulent wall jet. Comparisons between different experiments with the above configurations provided also information on the entrainment and mixing properties of each.

We aimed to understand the behaviour of turbulent jets incorporating the recent advances in non-homogeneous turbulence, structure function analysis, multifractal techniques and extended self-similarity. We focus special attention on correlations and structure function which are useful for energy spectra analysis.

In second part we showed that multi-fractal method allows investigating the turbulent and fractal structure of non homogeneous jets affected by different levels of turbulence and it can be useful to develop further multi-fractal techniques for environmental.

Future work involves further advanced research on this subject. Our plans include using laser methods LIF (Laser Induced Fluorescence) and PIV (Particle Image Velocimetry) available at our department for analysis of the jet's structure with video-camera visualization using DigImage software.

## **References**

- (1) R. Castilla Lopez (2001) "Simulación cinemática de flujo turbulento. Aplicación al estudio de la estructura de la turbulencia y de la difusión turbulenta", Doctoral thesis, Universitat Politècnica de Catalunya
- (2) J. G. Eriksson, R. I. Karlsson, J. Persson (1998) "An experimental study of a two-dimensional plane turbulent wall jet", *Experiments in Fluids* 25, 50-60
- (3) J. O. Hinze (1975) "Turbulence" 2<sup>nd</sup> edition, New York, McGraw-Hill cop.
- (4) G. H. Jirka (2004) "Integral Model for Turbulent Buoyant Jets in Unbounded Stratified Flows. Part I: Single Round Jet" *Environmental Fluid Mechanics* 4, pp. 1-56
- (5) K. Knowles, M. Myszko (1998) "Turbulence measurements in radial wall-jets" *Experimental Thermal and Fluid Science* 17, pp. 71-78
- (6) A. N. Kolmogorov (1941) "Local structure of turbulence in an incompressible fluid for very large Reynolds numbers" *Comptes rendus (Doklady) de l'Academie des Sciences de l'U.R.S.S.*, 31: 301-305
- (7) A. N. Kolmogorov (1962) "A refinement of previous hypotheses concerning the local structure of turbulence in a viscous incompressible fluid at high Reynolds number" *J. Fluid. Mech.* 13, pp - 82-85
- (8) B. E. Launder, W. Rodi (1983) "The turbulent wall jet – measurements and modelling" *Annual reviews of fluid mechanics*, vol. 15, pp. 429-459
- (9) E. J. List (1982) "Turbulent jets and plumes" *Annual review of fluid mechanics*, vol. 14, pp. 189 – 212
- (10) J. L. Lumley, A. M. Yaglom (2001) "A century of Turbulence", *Flow, Turbulence and Combustion*, 66: 241-286

- (11) O. B. Mahjoub (2000) "Non-local dynamics and intermittency in non-homogenous flows" Doctoral thesis, Universitat Politecnica de Catalunya
- (12) A. Platonov, A. Tarquis, E. Sekula and J. M. Redondo (2007) "SAR observations of vortical and turbulence in the ocean", *Models, Experiments and Computation in Turbulence*, R. Castilla, E. Oñate and J. M. Redondo (Eds.), CIMNE, Barcelona, Spain
- (13) N. Rajaratnam (1976) "Turbulent jets", Amsterdam (etc), Elsevier
- (14) H. Tennekes, J. L. Lumley (1972) "A first course in turbulence", The MIT Press
- (15) J. S. Turner (1973) "Buoyancy effects in fluids", Cambridge University Press
- (16) G. Voulgaris, J. H. Trowbridge (1997) "Evaluation of the Acoustic Doppler Velocimeter (ADV) for Turbulence Measurements", *Journal of Atmospheric and Oceanic Technology*, Volume 15